DOI: 10.1002/ejic.200600927

Synthesis and Oxidation of Vanadyl Complexes Containing Bispidine Ligands

Peter Comba,*[a] Shigemasa Kuwata,[a] Gerald Linti,[a] Máté Tarnai,[a] and Hubert Wadepohl[a]

Keywords: Peroxido complexes / Superoxido complexes / Rigid ligand / Bispidine

The reaction of 3-methyl-9-oxo-7-picolyl-2,4-di(2-pyridyl)-3,7-diazabicyclo[3.3.1]nonane-1,5-dicarboxylate (L^2) with vanadyl sulfate in methanol yields the purple complex $[V^{IV}{=}O(L^{2'})](ClO_4)_2$, where L^2 is hydrated to the corresponding 9-diol $L^{2'}$. The crystal structure of $[V^{IV}{=}O(L^{2'})](ClO_4)_2$ has a saturated coordination sphere with a long bond to the tertiary amine N7 *trans* to the oxido group (2.36 Å). Oxidation of $[V^{IV}{=}O(L^{2'})](ClO_4)_2$ with an excess of aqueous hydrogen peroxide yields the orange complex $[V^{V}{=}O(O_2)(L^{2'})]ClO_4$. This can be further oxidized with Ce^{4+} in MeCN at –40 °C to the unstable vanadium(V)-oxidosuperoxido complex $[V^{V}{=}O(O_2)(L^{2'})]^{2+}$, as shown by EPR spectroscopy. The X-ray crystal structure of $[V^{V}{=}O(O_2)(L^{2'})]ClO_4$ shows that the N7-pendant pyridine donor is dissociated and the V–N7 bond is elongated (2.56 Å). The O–O distance of the side-on bound peroxide in $[V^{V}{=}O(O_2)(L^{2'})]ClO_4$ is unexpectedly short (1.28 Å) and is therefore in the range which is typical for a superoxido group. However, the IR spectrum of $[V^{V}{=}O(O_2)(L^{2'})]ClO_4$ shows ^{18}O isotope shifts, which support the assignment as a peroxido complex, and this is also supported by EPR and UV/Vis spectroscopic analysis. The short O–O bond is attributed to a static disorder rather than to libration of the "non-rigid" peroxido group.

Introduction

Oxidation states up to +5 are accessible for vanadium, and in the high valent vanadium(IV) (d^1, vanadyl) and vanadium(V) (d^0, vanadate) forms the hard metal centers form stable oxido complexes. There is a considerable interest and activity in developing vanadium complexes as models for a variety of metalloenzymes, specifically for the mononuclear haloperoxidases, which catalyze the peroxide-dependent halogenation of organic substrates.[1,2] Vanadium(V) oxido-peroxido complexes have also been found to be catalytically active in the oxidation of organic substrates (e.g., epoxidation of alkenes and hydroxylation of alkanes and aromatic compounds).[3,4] In addition, mononuclear vanadyl(IV) and peroxidovanadium(V) complexes are known to have insulin-mimetic properties.[5,6]

Three pentadentate bispidine-based ligands with tertiary amine, pyridine, and phenolate donors have been used for the isolation and characterization of oxido- and peroxidovanadium(IV) and -vanadium(V) complexes (see Scheme 1). Upon complexation, the 9-keto group of the ligands is hydrated to the corresponding 9-diol, and in methanolic solution the hemiacetal structure (9-hydroxy-9-methoxy) can be formed; the hydrated diol ligands are denoted as $L^{1'}$, $L^{2'}$, and $L^{3'}$, respectively. Bispidine ligands are relatively soft and therefore prefer relatively large metal ions,[7] which means that they are not optimal for vanadium(IV/V) chemistry and quite rigorous methods have to be used for their preparation. Several methods have been reported for the preparation of vanadyl complexes;[8] of special interest are those for the synthesis of complexes with similar amine/pyridine-based ligands.[9]

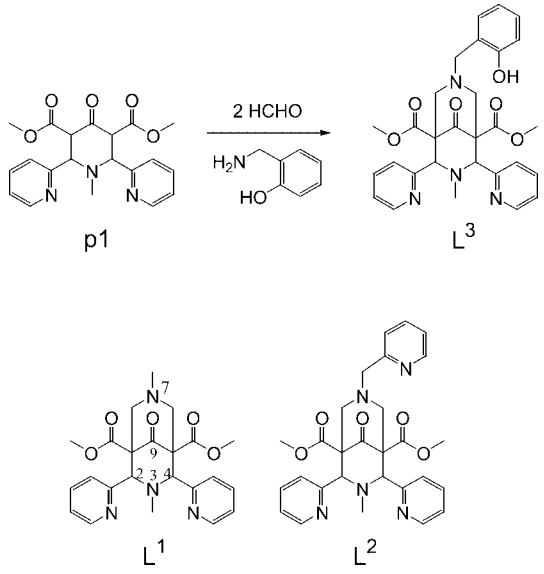

Scheme 1.

[a] Universität Heidelberg, Anorganisch-Chemisches Institut,
Im Neuenheimer Feld 270,
69120 Heidelberg, Germany
Fax: +49-6221-546617
E-mail: peter.comba@aci.uni-heidelberg.de

We report here the synthesis and properties of vanadium complexes of the three ligands shown in Scheme 1. Specifically, we have been interested in the structural and spectroscopic properties of the oxidovanadium(V) peroxide complex and the possibility of oxidizing it to the corresponding superoxide complex. Possible applications in the area of oxidation catalysis are briefly discussed on the basis of preliminary test reactions.

Results and Discussion

Synthesis and Structure of the Vanadyl Complexes

The vanadyl complexes with the pentadentate ligands L^2 and L^3 were prepared from vanadyl sulfate. These complexes are easily obtained from hot methanolic or acetonitrile (L^3) solutions (with addition of one equivalent of triethylamine to deprotonate the phenolic group donor). The complexes were purified by ion-exchange chromatography. Attempts to use vanadium(III) salts (chloride, acetylacetonate) did not produce any of the desired products. Interestingly, the method found to be successful for the pentadentate ligands did not succeed for the tetradentate ligand L^1. Treatment of L^1 with an ethanolic solution of [VO(OEt)$_3$] produced a deep-green solution after refluxing overnight, from which a dark green solid precipitated after several days in the refrigerator (4 °C). Characterization of the product confirmed the formation of the vanadyl complex of L^1 ([V=O($L^{1'}$)(OH$_2$)]$^{2+}$).

A plot of the molecular structure of [V^{IV}=O($L^{2'}$)](ClO$_4$)$_2$·H$_2$O, as determined by X-ray crystal structure analysis, is shown in Figure 1; the structural data are presented in Table 1. Only one of the two independent complex ions is discussed because they do not differ much in their structural parameters. The vanadyl ion coordinates to $L^{2'}$ in a distorted octahedral geometry. The vanadium center lies almost in the plane defined by Npy1, Npy2, and N3. The distance between vanadium and this plane is 0.074 Å, although the two pyridyl rings are twisted by 14.0° and 13.5° with respect to this plane. The length of the V=O bond (1.59 Å) is consistent with values found for other vanadyl complexes.[10] The V–N7 bond length (2.36 Å) is rather long for a V^{IV}–N_{amine} bond, whereas that of V–N3 (2.10 Å) is as expected.[11] The average V^{IV}–N bond length (2.15 Å) is ideal for the L^2 bispidine ligand cavity, which means that almost no strain is induced in the ligand by the vanadyl center.[7] Long bonds to N7 are quite common in bispidine coordination chemistry,[12–14] probably due to the bispidine-ligand-enforced angular distortion of the N7–V–O axis and, to a lesser extent, to π-bonding involving the two in-plane pyridine donors.[15] Long bonds in vanadyl complexes *trans* to the yl oxygen donor are also common, therefore the bispidine ligands L^2 and L^3, which enforce the yl oxygen group *trans* to N7, have a high complementarity with respect to the vanadyl fragment and form stable vanadyl complexes.

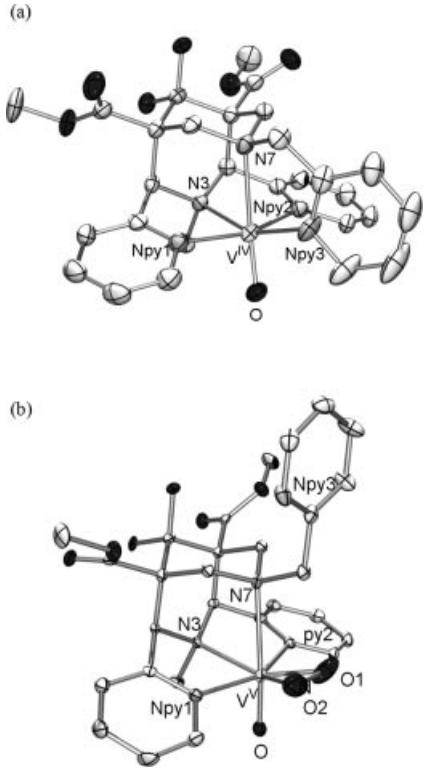

Figure 1. Molecular structures of [V=O($L^{2'}$)]$^{2+}$ (a) and [V=O(O$_2$)($L^{2'}$)]$^+$ (b). Displacement ellipsoids are scaled to 50% probability.

Table 1. Selected bond lengths and angles for [V=O(L^2)](ClO$_4$)$_2$·H$_2$O (a) and [V=O(O$_2$)(L^2)]ClO$_4$·H$_2$O (b).

	a	b
Distances [Å]		
V–N3	2.098(3)	2.192(2)
V–N7	2.364(3)	2.557(3)
V–Npy1	2.109(4)	2.112(3)
V–Npy2	2.097(4)	2.113(3)
V–Npy3	2.078(4)	–
V=O	1.589(3)	1.602(2)
$(V–N)_{av}$	2.149	2.244
V–O1	–	1.810(3)
V–O2	–	1.838(3)
O1–O2	–	1.281(5)
N3···N7	2.836(5)	2.909(3)
Npy1···Npy2	4.131(5)	4.087(3)
Angles [°]		
N3–V–N7	78.69(12)	75.07(9)
N3–V–Npy1	79.61(13)	75.95(10)
N3–V–Npy2	78.89(13)	74.62(10)
N3–V–Npy3	154.55(14)	–
N3–V=O	108.32(15)	98.34(11)
N7–V=O	172.70(15)	172.55(9)
Npy1–V–Npy2	158.28(13)	150.51(11)
Torsion angles [°]		
C1–C2–CA–Npy1	84.31(40)	89.77(34)
C5–C4–CA2–Npy2	–86.99(39)	–94.65(34)

Spectroscopy of the Vanadyl Complexes

The IR spectra for all complexes, as expected, have no Bohlmann band (ca. 2600 cm^{-1}), which typically appears for the metal-free bispidine ligand (interaction between the lone pairs of the tertiary amine nitrogen donors); this is usually missing when a metal is coordinated.[16] The vibrational band at 986 cm^{-1} in the spectrum of $[V^{IV}{=}O(L^{2'})](ClO_4)_2$ is assigned to the V=O stretching mode, and this is consistent with known five- and six-coordinate vanadyl complexes, where $\nu_{V=O}$ appears around 980 cm^{-1} and 950 cm^{-1}, respectively.[17,18] As expected from the structural data (see above) $[V^{IV}{=}O(L^{2'})](ClO_4)_2$, due to the long V–N7 distance, has a V=O stretching mode similar to that expected for a five-coordinate vanadyl complex.

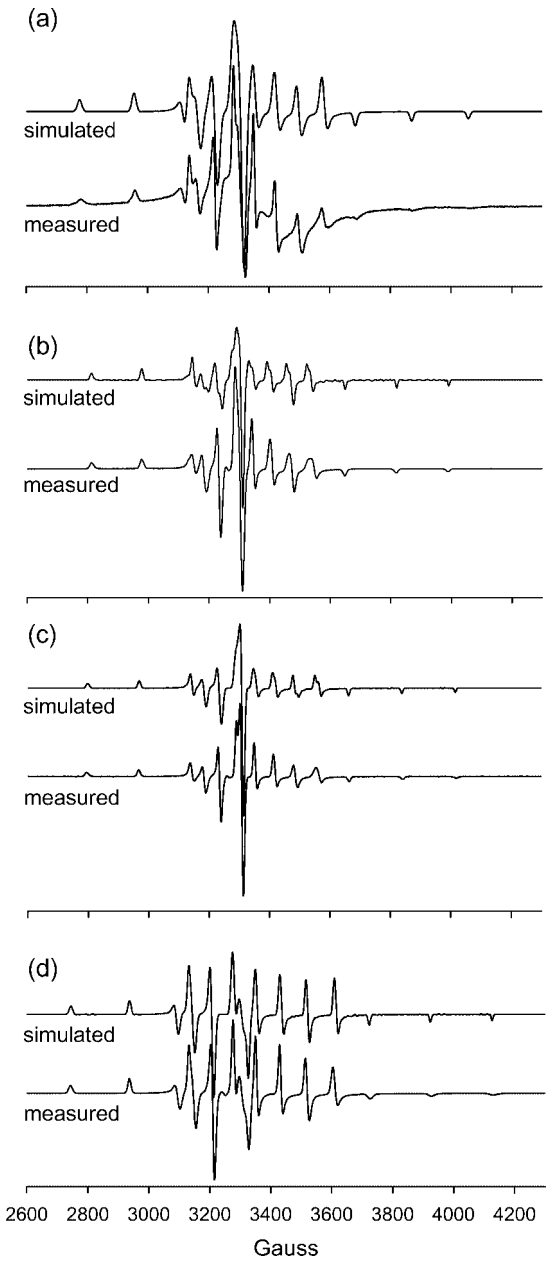

Figure 2. Experimental and simulated EPR spectra of $[V{=}O(L^{1'})]^{2+}$ (a), $[V{=}O(L^{2'})]^{2+}$ (b), $[V{=}O(L^{3'})]^{+}$ (c), and $[V{=}O(OH_2)_5]^{2+}$ (d) (dmf/H_2O, 2:1, 125 K, X-band).

The three d–d transitions expected for a distorted octahedral d^1 system are observed in the UV/Vis spectrum of $[V^{IV}{=}O(L^{2'})](ClO_4)_2$. The highest energy transition, which appears as a shoulder of the high intensity charge-transfer band at 363 nm, is assigned to the $d_{xy} \rightarrow d_{z^2}$ transition. Two weaker transitions at 514 and 695 nm are assigned to $d_{xy} \rightarrow d_{x^2-y^2}$ and $d_{xy} \rightarrow d_{xz,yz}$, respectively. A moderate ligand field in the expected range (D_q = 1950 cm^{-1}) emerges [$D_q(VOSO_4{\cdot}H_2O)$ = 1600 cm^{-1}] from this.[19,20] For $[V^{IV}{=}O(L^{3'})]^{+}$, only one dd transition is observed at 571 nm. The others are probably not resolved due to the strong charge-transfer transition at 386 nm, and this supports the coordination of the phenolate donor group.

The EPR spectra of the three bispidine vanadyl compounds and of the vanadyl aqua ion are shown in Figure 2. The spin-Hamiltonian parameters, obtained by spectral simulation,[21] are given in Table 2. The spectra are typical for d^1 vanadyl systems with a d_{xy} ground state and a compressed tetragonal geometry.[22–24] The trend of the *g*- and *A*-tensor parameters (in particular of the *z* components) with decreasing values along the series $L^2 > L^3 > L^1 > (H_2O)_5$ depends on the type of chromophore (N_aO_b, $a + b = 5$), and is consistent with the expected level of delocalization of the unpaired electron to the donor groups, with the softer N donors leading to more covalent interactions than the harder O donors.

Oxidation of the Vanadium(IV) Bispidine Complexes

The oxidation of a methanolic solution of $[V^{IV}{=}O(L^{2'})]^{2+}$ with a large excess of 30% aqueous H_2O_2 was studied by time-dependent UV/Vis/NIR spectroscopy. The series of spectra (see Figure 3) show a gradual decrease of the d–d transitions of the vanadyl complex (695 nm) and the appearance of a more intense single band at 429 nm (the color of the solution changes from light purple to orange). These changes indicate that metal-centered oxidation occurs. The reaction shows two isosbestic points at 390 and 547 nm and a pseudo-first-order behavior. The rate

Table 2. EPR parameters of the vanadyl complexes.[a]

	A_{xx} [10^{-4} cm^{-1}]	A_{yy} [10^{-4} cm^{-1}]	A_{zz} [10^{-4} cm^{-1}]	g_{xx}	g_{yy}	g_{zz}
$[V{=}O(L^2)]^{2+}$	–51	–50	–153	1.988	1.977	1.950
$[V{=}O(L^3)]^{+}$	–54	–55	–158	1.979	1.972	1.947
$[V{=}O(L^1)(OH_2)]^{2+}$	–60	–60	–166	1.977	1.977	1.943
$[V{=}O(OH_2)_5]^{2+}$	–68	–68	–178	1.977	1.972	1.932

[a] Obtained by simulation of the experimental spectra.[21]

of disappearance of the d–d band at 700 nm and increase of the charge-transfer band at 430 nm leads to a reaction rate, k_{obs}, of 1.02×10^{-3} s^{-1}. The product formed was purified by ion-exchange chromatography and characterized as a oxidovanadium(V) peroxide complex. The transition at 430 nm is assigned to a peroxide-to-vanadium charge-transfer transition. This is in the range typical for oxidovanadium(V) peroxide complexes.[8,30]

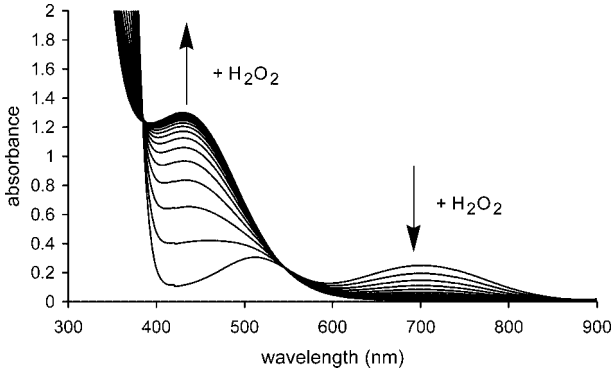

Figure 3. Time-dependent UV/Vis NIR spectra of the oxidation of $[VO(L^{2'})]^{2+}$ (11 mM MeOH) at 25 °C by H_2O_2 (170 equiv. of 30% aqueous solution) recorded at 5 min time intervals.

The CT band at 430 nm formed during oxidation is shifted to 456 nm in a much slower process (approx. one day). This is assigned to a rearrangement of an initially formed oxidohydroperoxido intermediate, which produces the oxidovanadium(V) peroxide complex (see Scheme 2).[4] This intramolecular rearrangement is expected to be a slow process because it involves ligand substitution at the vanadium(V) center. No intermediates were detected by EPR spectroscopy, which indicates that the first, relatively fast process is probably the oxidation of the V^{IV}=O complex and that no vanadyl peroxide intermediates can be trapped.

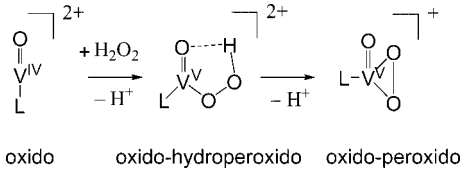

Scheme 2.

The oxidation products were analyzed with various oxidant concentrations, in a number of different solvents, and after quenching the reactions after various time intervals. Maximum yields of the vanadium(V) product were obtained with rather large amounts of H_2O_2 as oxidant (170 equiv.) and when the reaction was quenched after 2 h. When these reaction mixtures were left for two days, ESI mass spectrometry indicated that the orange product had completely decomposed (yellow solution). Aprotic solvents seem to lead to more side products than protic solvents, and the highest yields were obtained in MeOH and MeCN. This is not unexpected since vanadyl/H_2O_2 systems are known to produce OH radicals[25] and the yields of the vanadium(V) product seem to correlate with the ability of the solvent to quench these radicals.

Three transitions are found in the low energy part of the IR spectrum, at 890, 932, and 962 cm^{-1}. Based on published data, the absorption at 962 cm^{-1} can be attributed to the V=O stretching vibration. The other two are tentatively assigned to O–O modes. To confirm this assignment, an ^{18}O-labeling study was performed with $H_2{}^{18}O_2$ as oxidant (see Figure 4). In the IR spectrum of the $[V^{V}=O(^{18}O_2)(L^{2'})]^{+}$ complex, the transitions originally seen at 932 and 890 cm^{-1} are shifted to 887 and 850 cm^{-1}, respectively. These experimental isotope shifts are close to those expected theoretically. Similar isotope shifts are also observed in the nitrate salt of the complex.

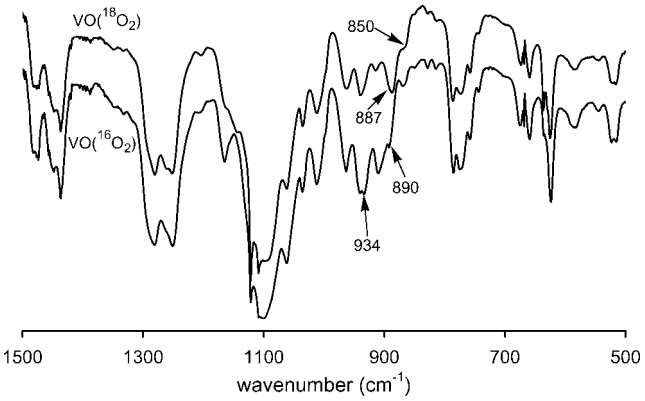

Figure 4. FT-IR spectra (KBr pellet) of $[V=O(O_2)(L^{2'})]^{+}$; top: synthesis with $H_2{}^{18}O_2$; bottom: synthesis with $H_2{}^{16}O_2$.

Single crystals of $[V^{V}=O(O_2)(L^{2'})]ClO_4 \cdot H_2O$ suitable for an X-ray structure determination were obtained by slow evaporation of the solvent (water/acetonitrile, 1:10). The resulting orange crystals are stable in air for several days. The structure of the cation $[V^{V}=O(O_2)(L^{2'})]^{+}$ is shown in Figure 1; selected geometric parameters are given in Table 1. The V–Npy1 and V–Npy2 distances are similar to the values determined for the corresponding vanadyl complex (see Table 1). The V–N3 distance is somewhat longer than in the vanadium(IV) complex and this may be due to the peroxido group, which leads to five in-plane donor atoms attached to the vanadium(V) center. This also leads to a smaller Npy1–V–Npy2 angle in the oxidovanadium(V) peroxide complex. The structure shows that the side-on coordination of the peroxido group requires the dissociation of the third pyridine group Npy3. As a result, there is a marked elongation of the V–N7 bond (2.56 vs. 2.36 Å) and, as a consequence, the distance between the two tertiary amino nitrogen donors increases from 2.84 to 2.91 Å. This value is very similar to that in the metal-free ligand L^1 (N3···N7 = 2.901 Å) and indicates that the oxidation of the vanadium center and the coordination of the peroxido group are assisted by the rigid bispidine ligand structure. The V=O distance, as expected, is rather insensitive to the oxidation state and coordination environment of vanadium.[10]

The description of the complex as an oxidovanadium(V) peroxide species is not unambiguous − it might alternatively be assigned as an oxidovanadium(IV) superoxide complex. There is a linear correlation between the O–O

stretching frequency and the bond length in this type of complexes:[26] peroxido complexes generally have O–O distances of 1.4–1.5 Å and O–O stretching frequencies of 1050–1200 cm^{-1}.[26] Therefore, judging from the apparent bond length in the crystal [1.281(5) Å] the assignment should rather be $[V^{IV}{=}O(O_2)(L^{2'})]^+$ (superoxide), while the IR spectra (see above) indicate that $[V^{V}{=}O(O_2)(L^{2'})]^+$ (peroxide) is the correct formulation. Close inspection of the crystal structure reveals much larger atomic displacement parameter (ADPs) for O1 and O2 than for the other oxygen, nitrogen, and carbon atoms. In addition, there is a systematic deviation of the shapes of the "thermal" envelopes for O1 and O2 from spherical (Figure 5). Normally, such effects can be attributed to thermally induced libration of "non-rigid groups".[27] Such libration leads to a systematic shortening of the apparent bond lengths between the affected atoms. This effect has indeed been observed in some η^2-O_2 metal complexes.[26] In the present case, the Hirshfeld Δ parameters indicate a highly correlated displacement of the O_2 moiety relative to the rest of the molecule. However, the diffraction data were collected at low temperature (100 K), which should greatly diminish the amplitude of librational motion. Indeed, attempts to model the effects by libration around the obvious axis joining V and the mid-point between O1 and O2 were unsuccessful. Dynamic effects (i.e. thermal motion) cannot be ruled out completely, but the ADPs also reflect static displacements of the atoms in many individual unit cells from their macroscopic space-averaged positions. We therefore tentatively assign the high ADPs of O1 and O2 to static disorder effects and do not see any particular significance in the apparently short oxygen–oxygen bond. In addition to the infrared spectroscopic data discussed above, there are no low intensity dd transitions in the 600–1000 nm range in the UV/Vis spectrum. Furthermore, the charge-transfer transition at 456 nm is in the area expected for vanadium(V) peroxide compounds.

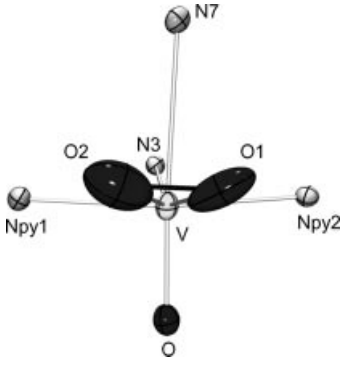

Figure 5. Displacement ellipsoids (50%) for the N_4OVO_2 core of the complex cation $[V{=}O(O_2)(L^{2'})]^+$.

It should be possible to oxidize oxidovanadium(V) peroxide complexes to the corresponding superoxido compounds.[28,29] Various oxidants were investigated (Co^{3+}, KO_2, Ce^{4+}), but only the preliminary experiments with Ce^{4+} were partially successful. Thus, addition of one equivalent of Ce^{4+} at –40 °C to an orange solution of $[V{=}O(O_2)$-$(L^{2'})]^+$ leads to a pale-yellow solution. Both Ce^{3+} and oxidovanadium(V) superoxide complexes are expected to be yellowish. Addition of H_2O_2 to this solution brings the orange color back. The EPR spectrum of the yellow solution shows a signal for Ce^{3+}. No other signals were observed after five minutes at 230 K. When the sample is left for a longer time at 230 K (10 min, see Figure 6) additional signals appeared, which were assigned to a VO^{2+} complex. These increase in intensity with longer reaction times whereas the intensity of the Ce^{3+} signal does not change. We tentatively interpret these observations as being due to the oxidation of $[V^{V}{=}O(O_2)(L^{2'})]^+$ (peroxide) to $[V^{V}{=}O(O_2)(L^{2'})]^{2+}$ (superoxide) and assume that the EPR signal of the superoxide is hidden under the Ce^{3+} signal. The vanadyl spectrum is a result of the decomposition of the metastable vanadium(V) superoxide complex to a vanadyl complex and dioxygen.

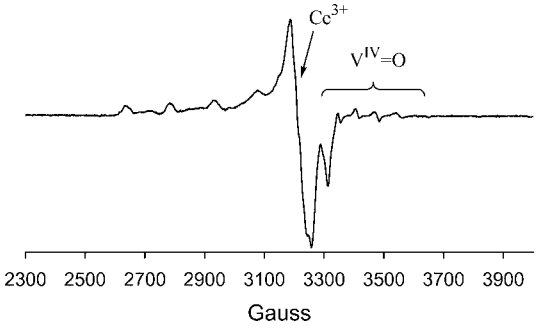

Figure 6. EPR spectrum of $[V^{V}{=}O(O_2)(L^{3'})]$ + 1 equiv. of Ce^{4+} (reaction for 10 min at 230 K; spectrum recorded at 100 K) in MeCN/dmf (1:2).

Reactivity

The vanadium(V) complexes were used for a number of catalytic oxidation test reactions (see Experimental Section). These include the bromination of phenol red (haloperoxidase test reaction)[30] and the oxidation of cyclohexene (epoxidation, hydroxylation).[4] There was no activity in the haloperoxidase test reaction and for cyclohexene oxidation the vanadium(V) complexes were also inactive. However, vanadyl complexes are also known to be able to oxidize olefins in the presence of H_2O_2.[31,32] Indeed, $[V^{IV}{=}O(L^{2'})]^{2+}$ has been shown to be able to oxidize cyclohexane but with a very low activity [0.7 mM catalyst, 7 mM H_2O_2, TON (cyclohexen-1-ol) = 0.1, TON (cyclohexen-1-one) = 0.3]. The vanadyl cations are believed to form hydroxyl radicals with H_2O_2,[25] and the allylic products probably emerge from these. The larger fraction of ketone product probably results from subsequent oxidation of the alcohol. The allylic products are likely to be, at least partially, the result of an autoxidation process involving dioxygen from air.[33] A possible reason for the low activity of the $[V^{IV}{=}O(L^{2'})]^{2+}/H_2O_2$ and $[V^{V}{=}O(O_2)(L^{2'})]^{+}/H_2O_2$ oxidation catalysis system is the saturated coordination sphere. A vacant coordination site has been proposed as

an active intermediate for the epoxidation process.[22] This might then explain the observed selectivity for allylic products.

Experimental Section

General: The ligands L^1,[34] L^2,[35] and L^3 [35] were synthesized according to known procedures.

$H_2{}^{18}O_2$ (90% ^{18}O enriched, 2% solution in $H_2{}^{16}O$) was obtained from ICON services, USA. Commercially available chemicals were used without further purification.

UV/Vis spectra were recorded with a V-570 Jasco instrument. ^1H and ^{13}C NMR spectra at 200.13 and 50.54 MHz, respectively, were recorded with a Bruker AS 200 spectrometer in $CDCl_3$, [D_6]-DMSO, or D_2O using TMS as an internal standard. Elemental analyses were obtained by the microanalytical laboratory of the chemical institutes of the University of Heidelberg. Mass spectra were measured with a Finnigan 8400 mass spectrometer. EPR spectra were recorded with a Bruker Elexsys E500 spectrometer at 110 K. Spectral parameters were determined by simulation using the program XSophe.[21] GC analyses were performed on a Varian 3900 gas chromatograph instrument equipped with a flame ionization detector, using a capillary column of Phenomenes Zebron ZB-1701 (length: 30 m; internal diameter: 0.25 mm). Temperature program: after 1 min, heating at a rate of 15 °C min^{-1} from 40 to 130 °C; after 11 min at this temperature, heating at a rate of 49 °C min^{-1} to 250 °C.

Crystal Structure Determination: Intensity data were collected with a STOE IPDS I or a Bruker AXS Smart1000 CCD diffractometer, and corrected for absorption and other effects.[36] Crystal data are compiled in Table 3. The structures were solved by direct methods and refined by full-matrix least-squares based on F^2. All non-hydrogen atoms were given anisotropic displacement parameters. Hydrogen atoms (except those of the solvent water molecule) were input in calculated positions. The calculations were performed using the programs SHELXS-86,[37,38] SHELXL-97.[39] Analysis of thermal motion was carried out with the program THMA11.[40]

CCDC-615579 ($[V^{IV}{=}O(L^{2'})](ClO_4)_2{\cdot}H_2O$) and -615580 ($[V^{V}{=}O(O_2)(L^{2'})]ClO_4{\cdot}H_2O$) contain the supplementary crystallographic data for this paper. These data can be obtained free of charge from The Cambridge Crystallographic Data Center via www.ccdc.cam.ac.uk/data_request/cif.

$[V^{IV}{=}O(L^{1'})](ClO_4)_2$: V_2O_5 (608 mg, 3.34 mmol) was added to MeOH (150 mL) and the resulting yellow suspension was refluxed overnight. Unreacted solid V_2O_5 was removed from the green suspension obtained by filtration, and a solution of L^1 (2.485 g, 5.67 mmol) in EtOH (100 mL) was added to the hot solution containing the $VO(OEt)_3$ product (0.5157 g, 5.67 mmol, 84.8%). The yellowish/greenish mixture was refluxed for 20 h, then $NaClO_4$ (1.593 g, 11.34 mmol) was added, and the solution was left at 4 °C overnight. The precipitate which formed was removed by filtration, washed with small portions of cold EtOH, and dried in vacuo. Yield: 260 mg (0.37 mmol, 7%). ESI-MS (MeOH): *m/z* 521.3 $[V^{IV}{=}O(L^1)(OH)]^+$, 539.3 $[V^{IV}{=}O(L^{1\prime})(OH)]^+$, 553.3 $[V^{IV}{=}O(L^1)(OH)(MeOH)]^+$. $C_{23}H_{26}Cl_2N_4O_{14}V$ (704.34): calcd. C 39.22, H 3.72, N 7.96; found C 39.30, H 4.07, N 8.30. IR (KBr): $\tilde{\nu}$ = 3436 br. s, 3078 w (CH), 2974 (CH_2), 1734 (C=O), 1604 m, 1474 m, 1444 m, 1270 m, 1090 (ClO_4), 964 m, 780 m, 624 m. UV (MeOH): λ (ε) = 370 nm (910 M^{-1} cm^{-1}), 470 (350, sh), 590 (190), 680 (190).

$[V^{IV}{=}O(L^{2'})](ClO_4)_2{\cdot}H_2O$: L^2 (1.00 g, 1.94 mmol) was dissolved in MeOH (30 mL) and a solution of $VOSO_4{\cdot}H_2O$ (0.49 g, 1.94 mmol)

Table 3. Crystal data for $[V^{IV}{=}O(L^{2'})](ClO_4)_2{\cdot}H_2O$ and $[V^{V}{=}O(O_2)(L^{2'})]ClO_4{\cdot}H_2O$.

	$[V^{IV}{=}O(L^{2'})](ClO_4)_2{\cdot}H_2O$	$[V^{V}{=}O(O_2)(L^{2'})]ClO_4{\cdot}H_2O$
Empirical formula	$C_{28}H_{31}Cl_2N_5O_{19}V$	$C_{28}H_{33}ClN_5O_{14}V$
Formula weight	863.42	749.98
Temperature [K]	293(2)	100(2)
λ [Å]	0.71073	0.71073
Crystal system	triclinic	triclinic
Space group	$P\bar{1}$	$P\bar{1}$
a [Å]	14.478(3)	8.8221(5)
b [Å]	14.707(3)	11.9404(7)
c [Å]	18.380(4)	16.1571(10)
α [°]	79.57(3)	71.039(1)
β [°]	74.30(3)	86.580(1)
γ [°]	70.01(3)	75.568(1)
Volume [Å^3]; Z	3523.6(12); 4	1571.79(16); 2
Density (calculated) [Mg m^{-3}]	1.628	1.585
Absorption coefficient [mm^{-1}]	0.524	0.480
Absorption correction	numerical	semi-empirical from equivalents
Min./max. transmission	0.722/0.798	0.942/0.988
F(000)	1772	776
Crystal size [mm^3]	0.619 × 0.596 × 0.471	0.125 × 0.125 × 0.025
θ range for data collection	1.7 to 24.04°	1.84 to 27.10°
Index ranges	$-16 \le h \le 16$ $-16 \le k \le 16$ $-20 \le l \le 20$	$-11 \le h \le 11$ $-14 \le k \le 15$ $0 \le l \le 20$
Reflections collected	22605	20669
Independent reflections	10390 [R_{int} = 0.0283]	6932 [R_{int} = 0.0504]
Goodness-of-fit on F^2	1.074	1.078
Parameters	991	447
Final R indices [$I > 2\sigma(I)$]	R_1 = 0.0616, wR_2 = 0.1770	R_1 = 0.0534, wR_2 = 0.1372
R indices (all data)	R_1 = 0.0759, wR_2 = 0.1881	R_1 = 0.0815, wR_2 = 0.1486
Largest diff. peak and hole [e Å^{-3}]	1.085/–1.328	1.178/–1.212

in MeOH (5 mL) was added. After refluxing for 1 h, the purple solution was evaporated to dryness and the product was separated on a CM Sephadex C-25 ion-exchange column with 0.1 M $NaClO_4$ as eluent. After partial solvent removal from the eluted purple band the product precipitated and was filtered and dried in vacuo. Yield: 0.81 g (0.99 mmol, 51%). ESI-MS (MeOH): *m/z* 291.5 $[V^{IV}{=}O\text{-}(L^2)]^{2+}$, 300.4 $[V^{IV}{=}O\ (L^{2'})]^{2+}$. $C_{28}H_{35}Cl_2N_5O_{17}V$ (835.42): calcd. C 40.25, H 4.22, N 8.38; found C 40.65, H 4.11, N 8.43. IR (KBr): $\tilde{\nu}$ = 3484 br. s, 3092 w, 2956 w, 1728 vs (C=O), 1608 s, 1479 m, 1437 w, 1286 s, 1281 w, 1253 w, 1205 w, 1098 vs, 1086 w, 986 w, 774 m, 658 w, 624 s, 538 w. CV (MeCN): E = –1.10 V (quasi rev.), –0.24 V (irrev.), 1.60 V (irrev.). UV (MeOH): λ (ε) = 254 nm (591 $M^{-1}cm^{-1}$), 363 (sh, 290), 514 (30), 695 (29)

$[V^{IV}{=}O(L^{2'})](BF_4)_2{\cdot}H_2O$: The reaction was performed in a similar fashion to that of $[V^{IV}{=}O(L^{2'})](ClO_4)_2{\cdot}H_2O$ but with 0.1 M $NaBF_4$ as eluent. Yield: 34%. ESI-MS: *m/z* 291.5 $[V^{IV}{=}O(L^2)]^{2+}$, 300.4 $[V^{IV}{=}O(L^{2'})]^{2+}$, 599.4 $[V^{IV}{=}O(L^2)(OH)]^{+}$. $C_{28}H_{35}B_2F_8N_5O_9V$ (810.13): calcd. C 41.50, H 4.35, N 8.65; found C 41.37, H 4.44, N 8.57. UV (MeOH): λ (ε) = 363 nm (290 $M^{-1}cm^{-1}$), 514 (30), 695 (29). IR (KBr): $\tilde{\nu}$ = 3432 br. s, 3112 w, 2962 w, 1732 s, 1608 m, 1482 m, 1438 s, 1284 s, 1258 s, 1060 vs, 776 m, 658 m.

$[V^{IV}{=}O(L^{3'})]Cl{\cdot}Et_3NHCl{\cdot}1.5H_2O$: A solution of $VOSO_4$ (239 mg, 0.942 mmol) in MeCN (40 mL) was added to a MeCN solution (50 mL) of L^3 (500 mg, 0.942 mmol), followed by triethylamine (131.1 µL, 0.942 mmol). The reaction mixture was refluxed for 1 h, whereupon the color of the solution turned deep green. After the solution had cooled down, water (200 mL) was added and the mixture was transferred to a CM Sephadex C-25 ion-exchange column. The blue band eluted with 0.1 M NaCl was collected. Yield: 513 mg (0.63 mmol, 67%). ESI-MS (MeOH): *m/z* 596.4 $[VO(L^3H_{-1})]^{+}$, 614.4 $[VO(L^{3'}H_{-1})]^{+}$, 628.4 $[VO(L^3H_{-1})(MeOH)]^{+}$. $C_{35}H_{50}Cl_2N_5O_{9.5}V$ (814.65): calcd. C 51.60, H 6.18, Cl 8.71, N 8.60; found C 51.47, H 5.97, Cl 8.83, N 8.79. UV (MeOH): λ (ε) = 386 nm (305 $M^{-1}cm^{-1}$), 571 (65), 766 (15, sh). IR (KBr): $\tilde{\nu}$ = 3422 br. s, 3070 w, 2980 w, 2950 w, 2676 m, 2624 m, 2498 w, 1734 vs (C=O), 1606 s, 1482 s, 1458 s, 1274 vs, 1100 vs, 974 s, 770 m, 622 m.

$[V^{V}{=}O(O_2)(L^{2'})]ClO_4{\cdot}H_2O$: 30% hydrogen peroxide (300 µL, 10 equiv.) was added to $[V^{IV}{=}O(L^{2'})](ClO_4)_2{\cdot}H_2O$ (0.25 g, 0.30 mmol) in MeOH (30 mL). After stirring at room temp. for 2 h, the formed orange product was purified on a CM Sephadex C-25 ion-exchange column. The orange band was collected by eluting with 0.1 M $NaClO_4$. After partial solvent removal, the precipitated orange solid was collected, washed with water, and dried in vacuo. Yield: 0.43 g (0.14 mmol, 47%). ESI-MS: *m/z* 632.3 $[VO(O_2)\text{-}(L^{2'})]^{+}$. $C_{28}H_{33}ClN_5O_{14}V$ (749.96): calcd. C 44.84, H 4.44, N 9.34; found C 44.59, H 4.55, N 9.20. ^{1}H NMR ([D$_6$]DMSO): δ = 7.23–9.92 (m, 12 H, Ar-H), 5.59 (s, 2 H, N-C*H*), 3.81 (s. 2 H, N-CH_2), 3.69 (s, 6 H, O-CH_3), 3.57 (s, 3 H, N-CH_3), 2.65 (d, 2 H, CH_2), 1.95 ppm (d, 2 H, CH_2). UV (MeOH): λ (ε) = 456 nm (137 $M^{-1}cm^{-1}$). IR (KBr): $\tilde{\nu}$ = 3378 s, 2952 w, 1734 vs, 1608 s, 1475 m, 1450 w, 1436 w, 1286 s, 1250 s, 1164 w, 1098 s, 1061 w, 1035 w, 1012 w, 963 w, 932 w, 890 w, 785 w, 771 w, 675 w, 623 m, 523 m.

$[V^{V}{=}O(O_2)(L^{2'})NO_3{\cdot}H_2O]$: The reaction was performed in a similar fashion to that of $[V^{V}{=}O(O_2)(L^{2'})]ClO_4{\cdot}H_2O$ but with 0.1 M $NaNO_3$ as eluent. ESI-MS(+): *m/z* 614.3 $[VO_3(L^2)]^{+}$, 632.4 $[VO_3(L^{2'})]^{+}$, 646.4 $[VO_3(L^2)(MeOH)]^{+}$; ESI-MS(–): *m/z* 738.2 $[VO_3(L^2)(NO_3)_2]^{-}$, 756.2 $[VO_3(L^{2'})(NO_3)_2]^{-}$, 770.2 $[VO_3(L^2)(NO_3)_2\text{-}(MeOH)]^{-}$. $C_{28}H_{33}N_6O_{13}V$ (712.51): calcd. C 47.20, H 4.67, N 11.80; found C 47.02, H 4.56, N 12.62. UV (MeOH): λ (ε) = 450 nm (350 $M^{-1}cm^{-1}$, sh). IR (KBr): $\tilde{\nu}$ = 3430 br. s, 3070 w, 2956 m, 1730 vs, 1606 s, 1480 m, 1436 m, 1384 s, 1278 m, 1250 m, 1204 w, 1158 m, 1106 m, 1060 s, 1032 m, 1006 w, 961 s, 937 m, 923 w, 830 w, 788 m, 674 m, 657 m, 585 m, 527 w.

$[V^{V}{=}O(^{18}O_2)(L^{2'})]ClO_4{\cdot}H_2O$: The reaction was performed in a similar fashion to that of $[V^{V}{=}O(O_2)(L^{2'})]ClO_4{\cdot}H_2O$ but with 2% $H_2{}^{18}O_2$ as oxidant. IR (KBr): $\tilde{\nu}$ = 3422 br. s, 3120 w, 2958 w, 2852 w, 1734 vs, 1608 m, 1482 m, 1436 m, 1282 s, 1252 s, 1098 vs, 1036 sh, 1012 m, 964 m, 936 w, 914 w, 886 m, 786 m, 772 m, 624 s.

$[V^{V}{=}O(O_2)(L^{3'}H_{-1})]Cl{\cdot}Et_3NHCl{\cdot}3.5H_2O$: A 30% (w/w) H_2O_2 solution (3.09 mL, 116 equiv.) was added to a solution of $[V^{IV}{=}O(L^{3'}H_{-1})]Cl{\cdot}Et_3NHCl{\cdot}1.5H_2O$ (211 mg, 0.259 mmol) in MeOH (40 mL). The reaction mixture was stirred for one week at room temp., whereupon the color turned orange. After dilution with water the mixture was transferred to a CM Sephadex C-25 ion-exchange column, and the main orange band was collected with 0.1 M NaCl as eluent. Yield: 64 mg (0.049 mmol, 19%). ESI-MS: *m/z* 629.3 $[V^{V}{=}O(O_2)(L^3H_{-1})]^{+}$, 647.4 $[V^{V}{=}O(O_2)(L^{3'}H_{-1})]^{+}$, 661.3 $[V^{V}{=}O(O_2)(L^3H_{-1})(MeOH)]^{+}$. $C_{53}H_{103}Cl_5N_8O_{13.5}V$ (1296.7): calcd. C 49.09, H 8.00, Cl 13.67, N 8.64; found C 49.09, H 7.35, Cl 13.67, N 8.66. IR (KBr): $\tilde{\nu}$ = 3430 br. s, 2977 w, 2942 w, 2678 m, 2623 w, 2604 w, 2495 m, 1734 m, 1607 m, 1473 m, 1442 m, 1279 br m, 1261 br m, 1106 w, 1036 w, 959 w. UV (MeOH): λ (ε) = 431 nm (240 $M^{-1}cm^{-1}$).

$[V^{V}{=}O(^{18}O_2)(L^{2'})]NO_3{\cdot}H_2O$: The reaction was performed in a similar fashion to that of $[V^{V}{=}O(O_2)(L^{2'})]NO_3{\cdot}H_2O$ but with 2% $H_2{}^{18}O_2$ as oxidant. IR (KBr): $\tilde{\nu}$ = 3420 br. s, 3080 br. m, 2952 m, 2852 w, 1732 s, 1608 m, 1480 w, 1436 m, 1384 vs, 1278 s, 1250 s, 1162 m, 1106 m, 1060 s, 1034 m, 1012 w, 962 m, 938 m, 886 s, 786 m sh, 776 sh, 758 m, 674 m, 658 m, 584 m, 517 m

Catalysis Test Reactions

Haloperoxidase Test: Bromination of the organic dye Phenol Red was carried out under conditions reported in the literature.[30]

Cyclohexene Oxidation: An H_2O_2 solution (0.3 mL; prepared by mixing 60 µL of 35% H_2O_2 and 10 mL of dry acetonitrile) was injected over 30 min with a syringe pump to a mixture of 2.1 µmol of vanadium complex and 2.1 mmol of cyclohexene in 2.7 mL of dry acetonitrile. After a given reaction time 1 mL of 6.8 mM naphthalene in acetonitrile was added as internal standard. The mixture was passed through a silica column, washed with ethyl acetate, and the eluate was directly analyzed by GC.[41]

Acknowledgments

Financial support by the German Science Foundation (DFG) is gratefully acknowledged.

[1] A. Butler, J. V. Walker, *Chem. Rev.* **1993**, *93*, 1937.
[2] D. Rehder, *Angew. Chem.* **1991**, *103*, 152; *Angew. Chem. Int. Ed. Engl.* **1991**, *30*, 148.
[3] A. Butler, M. J. Clague, G. E. Meister, *Chem. Rev.* **1994**, *94*, 625.
[4] H. Mimoun, L. Saussine, E. Daire, M. Postel, J. Fischer, R. Weiss, *J. Am. Chem. Soc.* **1983**, *105*, 3101.
[5] A. Shaver, J. B. Ng, A. Hall, B. S. Lum, B. I. Posner, *Inorg. Chem.* **1993**, *32*, 3109.
[6] P. Caravan, L. Gelmini, N. Glover, F. G. Herring, H. J. H. McNeill, S. J. Rettig, I. A. Setyawati, Y. E. Sun, S. Tracey, V. G. Yuen, C. Orvig, *J. Am. Chem. Soc.* **1995**, *117*, 127.
[7] C. Bleiholder, H. Börzel, P. Comba, R. Ferrari, A. Heydt, M. Kerscher, S. Kuwata, G. Laurenczy, G. A. Lawrance, A. Lienke, B. Martin, M. Merz, B. Nuber, H. Pritzkow, *Inorg. Chem.* **2005**, *44*, 8145.

[8] G. J. Colpas, B. J. Hamstra, J. W. Kampf, V. L. Pecoraro, *J. Am. Chem. Soc.* **1996**, *118*, 3469.
[9] H. Kelm, H.-J. Krüger, *Inorg. Chem.* **1996**, *35*, 3533.
[10] J. Selbin, *Coord. Chem. Rev.* **1966**, *1*, 293.
[11] H. Kelm, H.-J. Krüger, *Angew. Chem.* **2001**, *113*, 2406; *Angew. Chem. Int. Ed.* **2001**, *40*, 2344.
[12] P. Comba, M. Kerscher, M. Merz, V. Müller, H. Pritzkow, R. Remenyi, W. Schiek, Y. Xiong, *Chem. Eur. J.* **2002**, *8*, 5750.
[13] M. R. Bukowski, P. Comba, C. Limberg, M. Merz, L. Que Jr, T. Wistuba, *Angew. Chem.* **2004**, *116*, 1303; *Angew. Chem. Int. Ed.* **2004**, *43*, 1283.
[14] M. R. Bukowski, P. Comba, A. Lienke, C. Limberg, C. Lopez de Laorden, R. Mas-Balleste, M. Merz, L. Que Jr, *Angew. Chem.* **2006**, *118*, 3524; *Angew. Chem. Int. Ed.* **2006**, *45*, 3446.
[15] M. Atanasov, P. Comba, manuscript in preparation.
[16] F. Bohlmann, *Chem. Ber.* **1958**, *91*, 2157.
[17] X. Li, M. S. Lah, V. L. Pecoraro, *Inorg. Chem.* **1988**, *27*, 4657.
[18] J. A. Bonadies, C. J. Carrano, *J. Am. Chem. Soc.* **1986**, *108*, 4088.
[19] L. E. Orgel, *J. Chem. Phys.* **1955**, *23*, 1819.
[20] T. S. Piper, R. L. Carlin, *J. Chem. Phys.* **1960**, *33*, 1208.
[21] D. Wang, G. R. Hanson, *J. Magn. Reson. Ser. A* **1995**, *117*, 1.
[22] C. J. Ballhausen, H. B. Gray, *Inorg. Chem.* **1962**, *1*, 111.
[23] P. Comba, L. M. Engelhardt, J. M. Harrowfield, G. A. Lawrance, L. L. Martin, A. M. Sargeson, A. H. White, *J. Chem. Soc., Chem. Commun.* **1985**, 174.
[24] P. Comba, A. M. Sargeson, *Aust. J. Chem.* **1986**, *39*, 1029.
[25] R. Ma, A. Bakac, J. H. Espenson, *Inorg. Chem.* **1992**, *31*, 1925.
[26] C. J. Cramer, W. B. Tolman, K. H. Theopold, A. L. Rheingold, *Proc. Natl. Acad. Sci. USA* **2003**, *100*, 3635.
[27] J. D. Dunitz, E. F. Maverick, K. N. Trueblood, *Angew. Chem.* **1988**, *100*, 910; *Angew. Chem. Int. Ed. Engl.* **1988**, *27*, 880.
[28] R. C. Thompson, *Inorg. Chem.* **1982**, *21*, 859.
[29] R. C. Thompson, *Inorg. Chem.* **1983**, *22*, 584.
[30] G. J. Colpas, B. J. Hamstra, J. W. Kampf, V. L. Pecoraro, *J. Am. Chem. Soc.* **1994**, *116*, 3627.
[31] U. Schuchardt, M. C. Guerreiro, G. B. Shul′pin, *Russ. Chem. Bull.* **1998**, *47*, 247.
[32] D. M. Boghaei, S. Mohebi, *J. Mol. Catal. A: Chem.* **2002**, *179*, 41.
[33] H. Weiner, A. Trovarelli, R. G. Finke, *J. Mol. Catal. A: Chem.* **2003**, *191*, 217.
[34] U. Holzgrabe, E. Ericyas, *Arch. Pharm.* **1992**, *325*, 657.
[35] H. Börzel, P. Comba, K. S. Hagen, M. Merz, Y. D. Lampeka, A. Lienke, G. Linti, H. Pritzkow, L. V. Tsymbal, *Inorg. Chim. Acta* **2002**, *337*, 407.
[36] G. M. Sheldrick, University of Göttingen, Germany, **2004**.
[37] G. M. Sheldrick, University of Göttingen, Germany, **1986**.
[38] G. M. Sheldrick, *Acta Crystallogr., Sect. A* **1990**, *46*, 467.
[39] G. M. Sheldrick, University of Göttingen, Germany, **1997**.
[40] K. N. Trueblood, UCLA, CA, USA, **1987**.
[41] M. Merz, Dissertation, University of Heidelberg.

Received: October 1, 2006
Published Online: December 27, 2006

